17th World Conference on Earthquake Engineering, 17WCEE
Sendai, Japan - September 13th to 18th 2020

Evaluation of strain dependent coefficient of subgrade reaction of pile based on in-situ horizontal load test data with wide range diameter

S. Shimomura[(1)], Y. Suzuki[(2)]

[(1)] *Associate Prof., Nihon University, shimomura.shuichi@nihon-u.ac.jp*
[(2)] *Executive Research Engineer, Kajima Technical Research Institute, suzuki-y@kajima.com*

Abstract

Normally, a seismic design of pile foundations by static stress analysis, a model in which a pile is a beam and the beam and the ground are connected by multiple springs (coefficient of subgrade reaction k_h) is used as a practical design. The k_h calculated backward from the in-situ horizontal loading test results is used. This inversed k_h has little relation with ground strain level, and it is difficult to express continuously from the initial stiffness to the fracture of the ground. On the other hand, the coefficient of subgrade reaction k_h based on the theory of elasticity proposed by *A. B. Vesic* and modified by *A. J. Francis* used for dynamic stress analysis can be evaluated by the ground deformation coefficient in the initial state, but the agreement with the measured value remains unclear.

In this study, firstly pressuremeter test data used for ground deformation coefficient were collected and analyzed. And then the strain dependence of the ground deformation coefficient used for k_h evaluation was evaluated. Subsequently, in-situ horizontal loading test data of single piles with wide range pile diameter ranging from 250mm to 6600mm in width conducted were analyzed. Among them, k_h was evaluated from the analytical solution of a beam on the elastic multiple springs for the data of 22 cases of sandy soil ground and 17 cases of cohesive soil ground with uniform surface layer and sufficient ground survey results. Based on the inversed k_h, the evaluation method of k_h from the initial stiffness of the ground to the fracture considering the strain level of the ground was examined. Following conclusions were obtained.

1) A method for assessing the strain dependence of the ground deformation coefficient, which is employed in the assessment of the coefficient of subgrade reaction k_h, was determined. In addition, a ground deformation coefficient assessment independent of the soil type was performed by adopting shear wave velocity.
2) With regard to the non-linearity of the k_h, the fact that continuous changes with small variation could be assessed using the pile displacement/pile diameter, and the fact that the strain level of the ground could be considered throughout, were clarified.
3) An assessing method for k_h continuously from small strain to large strain, that can be used in dynamic analysis, with the springs proposed by *Francis* based on the theory of elasticity and with expanded hyperbolic model, was proposed.

Keywords: Single pile; Coefficient of subgrade reaction; Horizontal load test; Shear wave velocity, Pressuremeter test

1. Introduction

Normally, a seismic design of pile foundations by static stress analysis, a model in which a pile is a beam with flexural stiffness and the beam and the ground are connected by multiple springs (coefficient of subgrade reaction k_h) is used as a practical design. *Vesic*[1] and *Francis*[2] proposed a method for assessing k_h as a function of the ground deformation coefficient, pile width, and the flexural stiffness of the pile, based on the theory of elasticity. *Yoshinaka*[3] proposed an assessment method that compares the results of the horizontal load test of pile and depends on the ground deformation coefficient and pile width, based on a plate loading test in the horizontal direction and the theory of elasticity. In addition, based on the theoretical solution of a beam on an elastic bearing that considers a uniform ground and a long pile (hereinafter, theoretical solution[4,5]), it is demonstrated that in the k_h, which is assessed from an inverse analysis of the horizontal load test results (hereinafter, inversed k_h), the pile body is inversely proportional to half the power of the ground surface displacement within the elasticity range[6].

In the Recommendations for Design of Building Foundations[4] (hereinafter, the Recommendations) employed in Japan, a method utilizing the k_h, which serves as the reference level and is calculated from the ground deformation coefficient and pile diameter (hereinafter, reference coefficient of subgrade reaction k_{h0}), and non-linearity in accordance with the non-dimensional horizontal displacement of the pile, is suggested for assessing the k_h. In the k_{h0}, the horizontal displacement of the pile at the ground surface position (hereinafter, reference displacement) is 1cm. With regard to non-linearity, it is recommended that the displacement be assessed using a linear profile up to 0.1cm and a non-linear profile that is inversely proportional to half the power of the displacement at ≥ 0.1cm, until the horizontal subgrade reaction attains the ultimate value as shown in Fig.1.

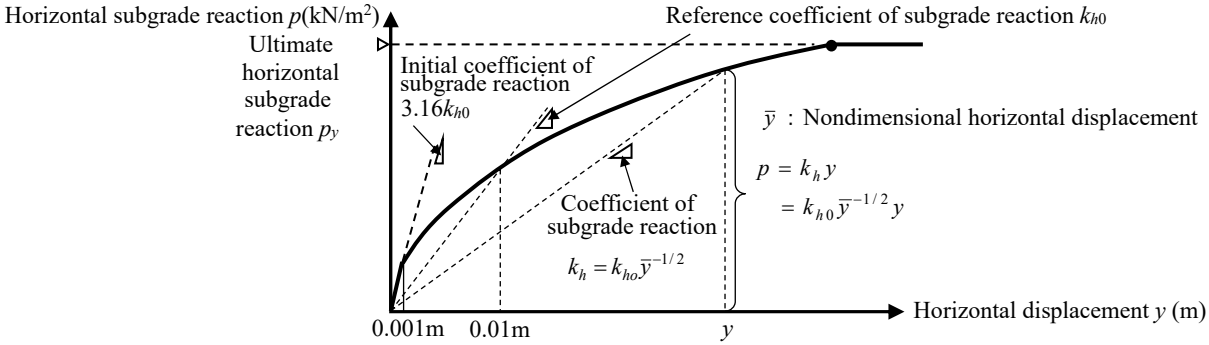

Fig.1 Evaluation of subgrade reaction coefficient based on the Recommendations

The equation for the k_{h0} in the Recommendations is derived using the ground deformation coefficient, obtained from the pressuremeter test[3]. However, the compressive strain of the ground used to evaluate this deformation coefficient E_b is several percent, and varies greatly depending on the test. Moreover, in the horizontal load test of the pile, the larger the pile diameter, the farther the stress or displacement inside the ground is transmitted in both the depth and the pile front. Consequently, the average strain of the pile front ground, during the pile head displacement of 1cm differs depending on the pile diameter, and any agreement with the pressuremeter test is uncertain. In other words, with regard to the k_h in the Recommendations, the agreement with the strain level of the ground is unclear, and it is difficult to claim that it has been continuously extracted from the initial stiffness of the ground to failure. Contrarily, in dynamic stress analysis, non-linearity has been assessed by using a continuous k_h as proposed by *Francis*, based on the theory of elasticity with a hyperbolic model, but the agreement with the measured value remains unclear.

Accordingly, in this paper, a method for assessing k_h from small displacement to large displacement is investigated using an examination of the effects of the strain level of the ground with pressuremeter test and an inversed analysis of horizontal load test results with the theoretical solution.

2. An assessment of the ground deformation coefficient that considers the strain level of the ground

In the assessment of the horizontal resistance of the pile in the Recommendations, the reference coefficient of the subgrade reaction k_{h0} of a single pile is calculated using Eq. (1).

$$k_{h0}=80E_S(B/B_0)^n \tag{1}$$

Here, k_{h0}(kN/m^3) is the reference coefficient of the subgrade reaction; E_S(kN/m^2) is the ground deformation coefficient; B(m) is the pile diameter; B_0 is the pile diameter that serves as the reference level (0.01m); n is the index-related pile diameter dependency, which is -3/4 in the Recommendations. In the Recommendations, Eq. (2) is used, if the ground deformation coefficient E_S is assessed from the N-value.

$$E_S=700N \tag{2}$$

Fig.2 shows the relationship between the ground deformation coefficient E_b, which is calculated from the pressuremeter test, and the N-value and unconstrained compressive strength q_u. In the same figure, the

power approximation equation for each data group based on the least-squares method, and the correlation coefficient R thereof, are both noted. Although there is little data for q_u and it is difficult to make a judgment, the relationship between E_b and the N-value varies greatly and this variation is more significant in the case of cohesive soil, where the graph slope differs, along with the fact that Eq. (2), which is used in the Recommendations, assigns a low value in sandy soil and cohesive soil, whose N-values are low.

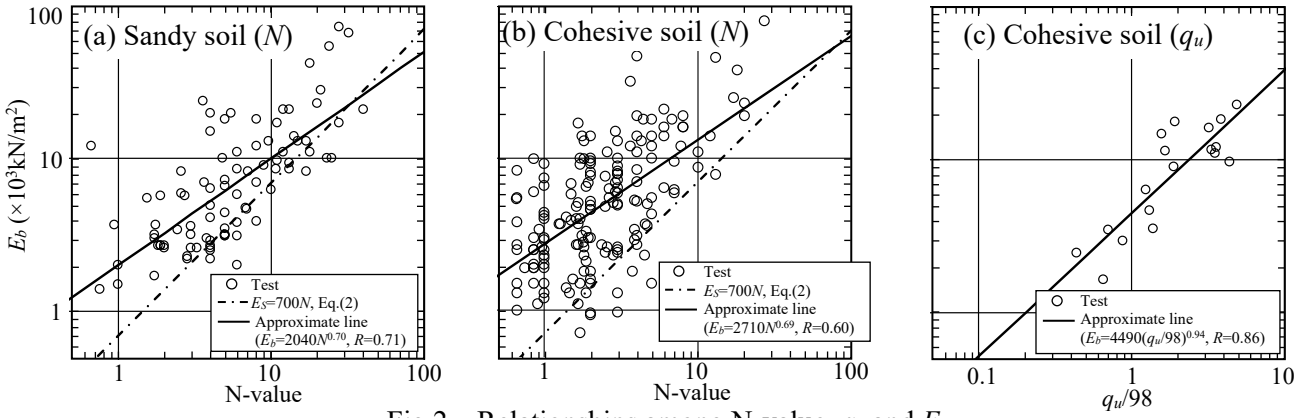

Fig.2 Relationships among N-value, q_u and E_b

Fig.3 shows the relationship between the radial strain ε_r[9,10] of the hole wall position that is employed in the assessment of E_b obtained in the pressuremeter test results, and the N-value and the unconstrained compressive strength q_u, used in Fig.2. The averages for each data group are shown by a broken line. With regard to the strain of the ground in the pressure meter results, there is great variation, when the N-value is small, and this may be one of the reasons for the variation that was confirmed in Fig.2.

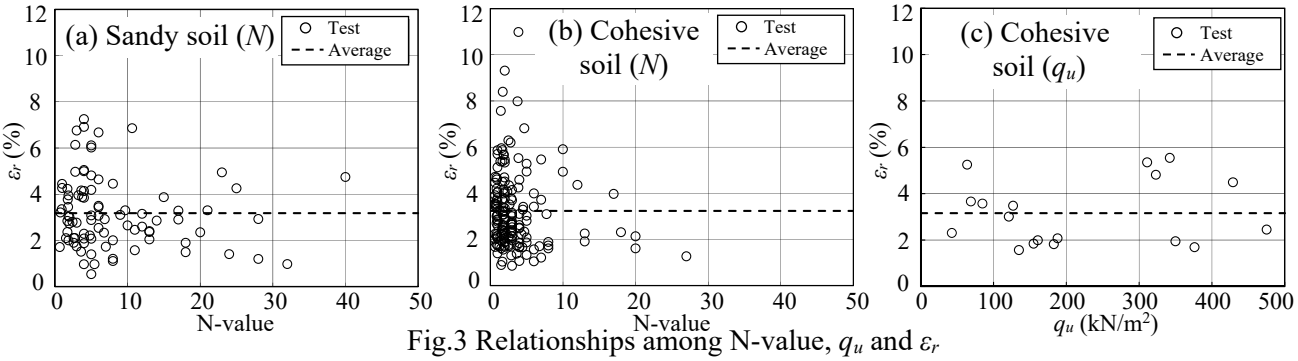

Fig.3 Relationships among N-value, q_u and ε_r

Fig.4 shows the relationship between the ε_r and the E_b, by comparing previous strain-dependent curves[11-13] that were employed in dynamic deformation tests. Since the range of the average $\pm\sigma$ (σ=standard deviation) is shown in reference [12], the scope of $\pm\sigma$ was known. For the vertical axis the stiffness reduction rate E_b/E_0, wherein E_b is divided by the initial deformation coefficient E_0 (calculated in Eq. (3) with the shear wave velocity V_S), and the stiffness reduction rate E_d/E_0 (calculated from previous dynamic deformation tests) were used, while for the horizontal axis the ε_r and the axial strain ε_a of the dynamic deformation tests were used. Since there is little information available for the employment of PS logging and pressuremeter tests at the same place, V_S was estimated from the N-value and q_u using Eqs. (4)-(6). In Eqs. (4)-(5), N-values of less than 1, which exceed the scope of application here, were employed by extrapolation.

$$E_0=2G_0(1+\nu)=2(1+\nu)\rho V_S^2 \quad (3)$$

(Sandy soil) $$V_S=80N^{1/3} \quad (4)$$

(Cohesive soil) $$V_S=100N^{1/3} \quad (5)$$

(Cohesive soil) $$V_S=134(q_u/98)^{0.443} \quad (6)$$

Here, G_0(kN/m^2) is the initial shear stiffness; v is Poisson's ratio (assumed to be 0.5); V_S(m/s) is the shear wave velocity; ρ(t/m^3) is the unit volume mass (sandy soil: 1.8, cohesive soil: 1.5); q_u(kN/m^2) is the unconstrained compressive strength. In addition, since the previous stiffness reduction rate (based on the relationship between the shear stiffness and the shear strain) was based on an undrained cyclic shear test of saturated soil, as shown in Fig.4, by converting the shear strain γ into the axial strain ε_a, assuming that Poisson's ratio is 0.5. All of the previous relationships were also extrapolated to a region that exceeds the scope of the test data, shown in each item in the references. From Fig.4, a tendency for the stiffness to decrease with increasing strain can be seen in the relationship of the E_b/E_0 and the ε_r. However, this does not necessarily agree with the dynamic deformation test, due to the fact that the ε_r is subject to the effects of local ground deformation in the vicinity of the loading face, and the definition of the strain is different from the strain of the dynamic deformation test.

Accordingly, the power approximation equation, for each data group based on the least-squares method in Fig.4, was employed, and the deformation coefficient E_b was converted into E_b' (equivalent to 3% of the average value of the ε_r shown in Fig.3), as shown in Fig.5, which demonstrates the results calculated using Eqs. (3)-(6) and the relationship between the power approximation equation based on the least-squares method and the -σ and -2σ thereof, as well as the relationships between Eqs. (2). Compared to Fig.2, the correlation coefficient R of the power approximation equation is increased as shown in Fig.5, and the slope of the power approximation equation is approximately congruent to the correlation calculated in Eq. (3) (from the shear wave velocity). Moreover, when the slope of the power approximation equation in the vicinity of the center of the data is compared by a line that conforms to Eqs. (3)-(6), E_b' (which is calculated from the power approximation equation) is equivalent to E_0/17 (N-value) in sandy soil, and E_0/18 (N-value) and E_0/18 (q_u) in cohesive soil, compared to E_0, which is obtained from Eqs. (3)-(6).

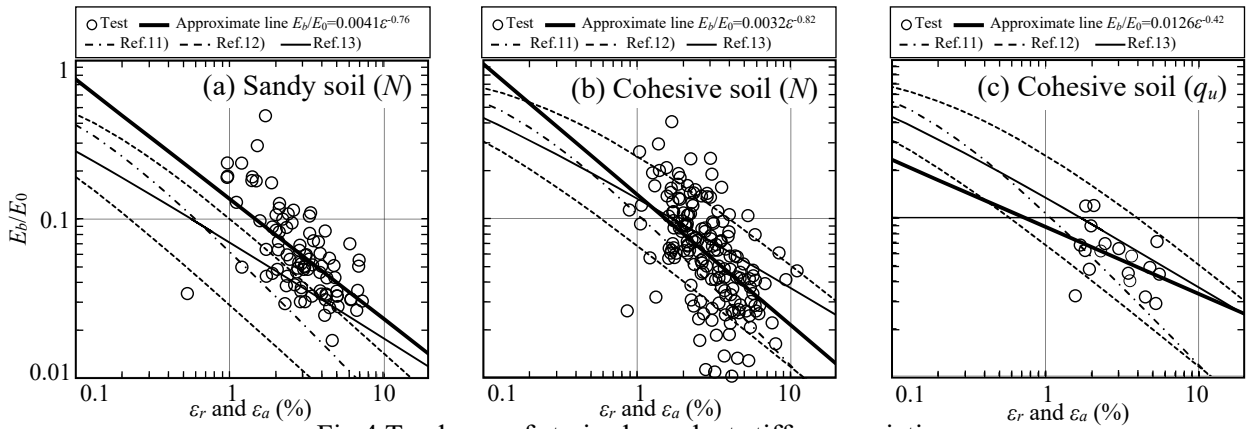

Fig.4 Tendency of strain-dependent stiffness variations

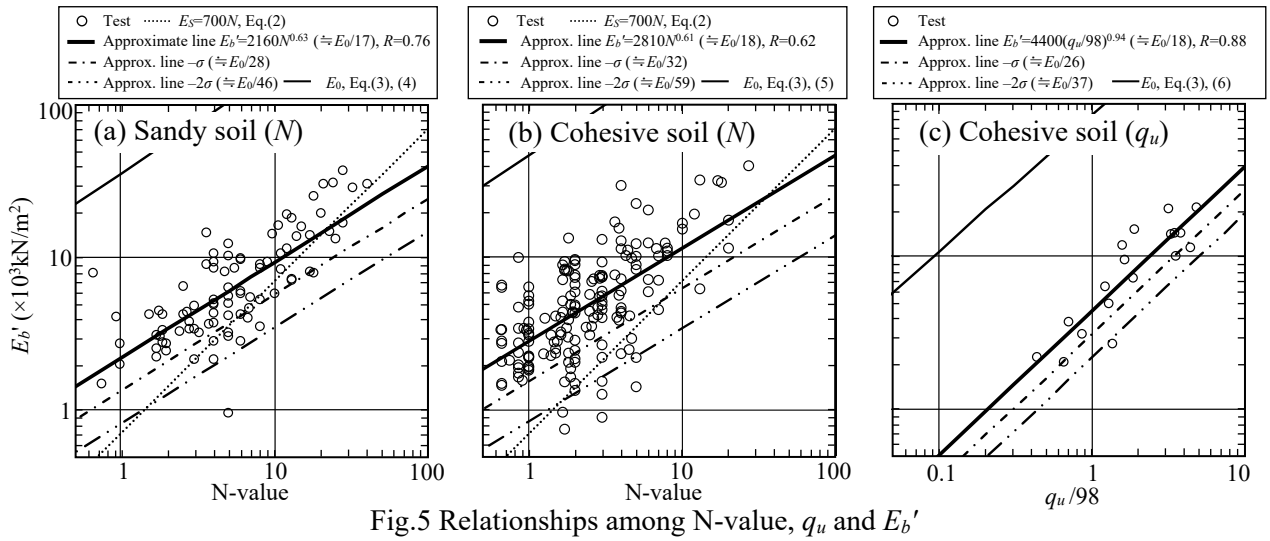

Fig.5 Relationships among N-value, q_u and E_b'

Thus, even though there may be a variation, depending on the data volume or the manner in which the line is drawn, an average calculation of E_b', estimated from the pressuremeter test by lowering the deformation coefficient E_0 (which is calculated from the shear wave velocity), was about 1/18, irrespective of the soil type.

3. Horizontal load test and pile diameter dependence of inversed k_h

The inversed k_h is calculated from the inverse analysis of the pile head load-pile head displacement relationship of the horizontal load test results, based on the theoretical solution. The method for setting the reference coefficient of the subgrade reaction k_{h0} and the reliance on the reference displacement, pile diameter and ground surface displacement, which are employed in the assessment of the former, were examined.

Table 1 lists[7,8] the horizontal load test results. We revised the data from the literature, excluding one test each for both kinds of soil. The pile head constraining condition, in all the tests conducted in Japan, is that of a rotatable single pile. If the figures for the load test results and the ground research results of the pile were not specified, then figures from the graphs were used.

In cohesive soil, we selected test results for which the unconstrained compressive strength q_u of the ground and the N-values are obtained (barring one part). The average value of the range of the reciprocal ($1/\beta$), of the characteristic value β of the pile from the ground surface (when the ground surface displacement of the horizontal load test was 1cm), was used for the N-value, q_u, and shear wave velocity V_S as shown in Table 1. Since there were no data for the V_S in the tests in question, the V_S was calculated using Eqs. (4)-(6) from the N-value and unconstrained compressive strength q_u of each depth, after which it was averaged.

The soil composition of the surface layer is relatively simple to model but in some parts, cohesive soil is inserted in the sandy soil and vice-versa, in a range of $1/\beta$. Accordingly, pattern division was performed for each layer of thickness of the sandy soil and the cohesive soil in the assessment of the ground deformation coefficient. First of all, in the case of sandy soil, as shown in Fig.6, many soils have an SI pattern, which does not contain a cohesive soil layer in a range up to $0.1/\beta$. In an SII pattern, the effects of the cohesive soil layer were judged to be small and were disregarded. In an SIII pattern in which the total cohesive soil layer thickness was $0.1/\beta$–$0.33/\beta$, the deformation coefficient was calculated from the N-value, including that for cohesive soil. When the sum of the cohesive soil layer thickness was $\geq 0.33/\beta$, it was excluded from the targets of examination. Almost all layer thicknesses exhibited a CI pattern in cohesive soil, and some of the sandy soil layer thicknesses had a CII pattern of $\leq 0.1/\beta$, but the effects were judged to be small and were disregarded, as in the case of sandy soil. None of the samples had a CIII pattern.

Fig.7 shows the relationship between the pile head horizontal load and the pile horizontal displacement at the loading point position. If the relationship between the pile head horizontal load and the pile horizontal displacement at the loading point position was not indicated in the reference, then an inverse calculation was performed using the theoretical solution (discussed below). In the subsequent analysis, the data for which the pile body was within the elasticity range was taken to be the object with reference to the descriptions in the literature, but if it was unclear whether there was any pile body yield from the horizontal load test, the simulation analysis results in Chapter 5 (discussed below) were used as a reference.

In the theoretical solution, the displacement y_{top}(m) at the loading point position of the pile is expressed by Eq. (7). Since βL (where β is the characteristic value of the pile; and L is the pile length) exceeded 2.25 in all of the test data, and they were determined to be piles of adequate length, it was judged that a theoretical solution that considered only the bending deformation could be applied.

$$y_{top} = \frac{(1+\beta h)^3 + 1/2}{3EI\beta^3} H + \frac{(1+\beta h)^2}{2EI\beta^2} M_{top} \tag{7}$$

$$\beta = \sqrt[4]{\frac{k_h B}{4EI}} \tag{8}$$

Table 1 Outline of past horizontal load tests of single pile

(a) Sandy soil deposit[7]

No.	Pile			Ground properties				Bending moment data
	Diameter (mm)	Type	Length (m)	Soil type	N value※)	Vs (m/s)	Pattern (Fig.6)	
S1	400	Concrete filling steel pipe	15.0	Fine sand	12	183	S Ⅰ	
S2	508	Steel pipe	8.0	Sand with gravel	3	115	S Ⅲ	
S3	508	Steel pipe	8.0	Sand with gravel	3	113	S Ⅲ	
S4	600	Hybrid steel pipe with soil cement	24.1	Sand with gravel	5	137	S Ⅰ	
S5	609.6	Steel pipe	14.7	Fine sand	5	137	S Ⅱ	
S6	609.6	Steel pipe	12.6	Fine sand	5	137	S Ⅱ	
S7	609.6	Steel pipe	24.0	Fine sand	12	178	S Ⅰ	✔
S8	800	Hybrid steel pipe with soil cement	25.8	Sand	3	113	S Ⅰ	
S9	800	Steel pipe	26.4	Fine sand	7	153	S Ⅲ	
S10	914.4	Steel pipe	26.0	Sand	3	111	S Ⅰ	✔
S11	914.4	Steel pipe	26.0	Sand	3	111	S Ⅰ	✔
S12	914.4	Steel pipe	26.0	Sand	3	113	S Ⅰ	
S13	1000	Steel pipe	46.0	Fine sand	10	158	S Ⅰ	✔
S14	1072.2	Steel pipe	19.5	Sand	5	135	S Ⅰ	
S15	1072.2	Steel pipe	19.5	Sand	5	135	S Ⅰ	
S16	1200	Cast-in-place concrete pile	21.6	Fine sand	16	203	S Ⅰ	✔
S17	2200	Cast-in-place concrete pile	40.0	Sand	5	133	S Ⅲ	
S18	2200	Cast-in-place concrete pile	70.0	Sand	5	134	S Ⅲ	
S19	3000	Cast-in-place concrete pile	70.0	Sand	6	144	S Ⅲ	
S20	2200	Cast-in-place concrete pile with rectangular section (Short side width : 600mm)	19.7	Sand	9	167	S Ⅰ	✔
S21	4400	Cast-in-place concrete pile with rectangular section (Short side width : 600mm)	19.7	Sand	9	166	S Ⅰ	✔
S22	6600	Cast-in-place concrete pile with rectangular section (Short side width : 600mm)	19.7	Sand	9	166	S Ⅰ	✔

(b) Cohesive soil deposit[8]

No.	Pile			Ground properties					Bending moment data
	Diameter (mm)	Type	Length (m)	Soil type	q_u※) (kN/m^2)	N value※)	Vs (m/s)	Pattern (Fig.6)	
C1	250	H-shaped steel pile	5.5	Loam	88	3	127	C Ⅰ	✔
C2	400	PC	25	Clay	30	0	79	C Ⅰ	
C3	400	Concrete filling steel pipe	18	Sandy silt	60	2	107	C Ⅰ	
C4	400	Prestressed concrete pile	22	Loam	234	3	195	C Ⅰ	
C5	600	PRC	18	Loam	24	0	71	C Ⅰ	
C6	600	PC	10	Clayey silt	27	2	75	C Ⅰ	
C7	600	SC	36	Silty clay	40	0	89	C Ⅰ	
C8	609.6	Steel pipe	28.7	Peat	18	—	63	C Ⅰ	✔
C9	609.6	Steel pipe	28.7	Peat	18	—	63	C Ⅰ	
C10	609.6	Steel pipe	18	Loam	24	0	71	C Ⅰ	✔
C11	1000	Steel pipe	17.5	Tuffaceous clay	57	5	105	C Ⅰ	✔
C12	1000	Concrete filling steel pipe	23.5	Sandy silt	60	2	107	C Ⅰ	✔
C13	1000	Concrete filling steel pipe	21	Sandy silt	60	2	107	C Ⅰ	
C14	1524	Steel pipe	43	Clay	20	–	66	C Ⅱ	
C15	1548	Cast-in-place concrete pile	30	Clay	65	1	111	C Ⅰ	✔
C16	2000	Cast-in-place concrete pile	30	Clay	65	1	111	C Ⅰ	
C17	2200	Cast-in-place concrete pile with rectangular section (Short side width : 600mm)	16.5	Loam	160	4	165	C Ⅰ	

※) Average from 0m to 1/β m depth

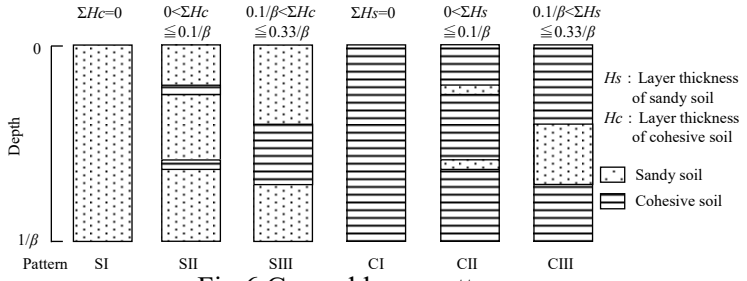

Fig.6 Ground layer pattern

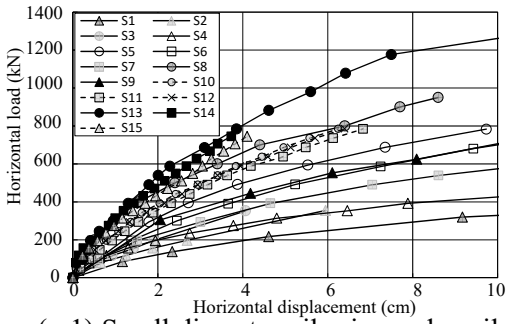

(a-1) Small diameter piles in sandy soil

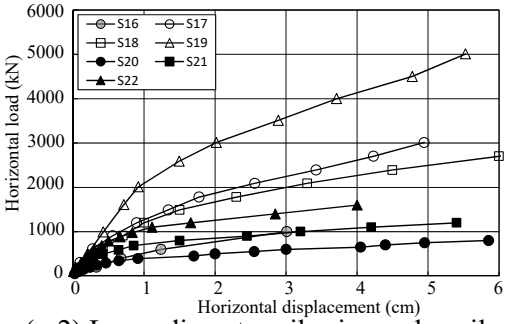

(a-2) Large diameter piles in sandy soil

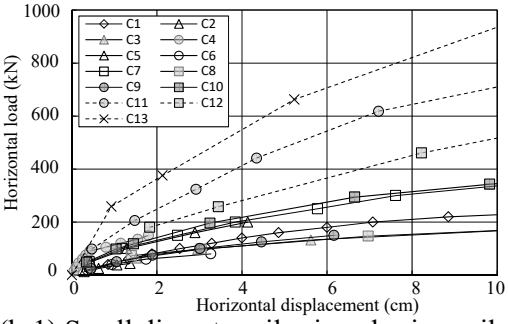

(b-1) Small diameter piles in cohesive soil

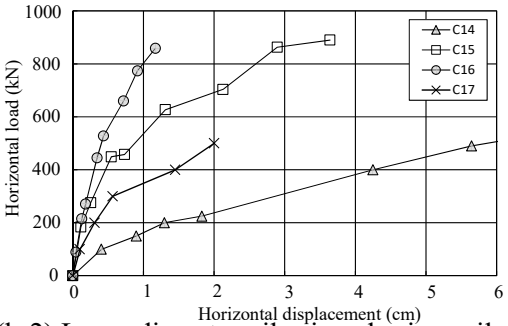

(b-2) Large diameter piles in cohesive soil

Fig.7 Relationships between horizontal load and horizontal displacement at pile head

Here, h(m) is the distance from the ground surface to the loading point; H(m) is the loading horizontal force; M_{top}(kN・m) is the bending moment of the loading point position; k_h(kN/m^3) is the coefficient of subgrade reaction; B(m) is the pile diameter; E(kN/m^2) is Young's modulus of the pile; and I(m^4) is the moment of inertia of area of the pile. The values described in each item in the reference were used for Young's modulus and the moment of inertia of the area of the pile. If Young's modulus was not indicated in the reference, it was assumed that the concrete was 2.05×10^7 kN/m^2 and the steel material was 2.05×10^8 kN/m^2. Since the target tests involved pile head rotatable conditions, M_{top} was set at zero, and an inversed k_h

was used for the k_h that fits the pile head load-pile head displacement of the horizontal load test by a convergent calculation employing the theoretical solution. In addition, the pile displacement y(m) at the ground surface position is calculated in Eq. (9).

$$y = \frac{1+\beta(h+h_0)}{2EI\beta^3}H \tag{9}$$

Here, $h_0=M_{top}/H=0$. In the horizontal resistance calculation equation in the Recommendations, the k_{h0} of a single pile is assessed by Eq. (1). In this chapter, the deformation coefficient that is adopted in Eq. (1) was calculated in Eq. (10), based on the examination results in Chapter 2.

$$E_S=E_0/18 \tag{10}$$

E_0 is calculated by Eq. (3) with the V_S shown in Table 1, which is calculated in Eqs. (4) and (6).

Relationship between the inversed k_h/estimated k_{h0}, which is calculated from Eqs. (1)-(2), and pile displacement at ground surface (hereinafter pile head displacement) is shown in Fig.8. The data for which the N-value was ≤ 0.5 was excluded from the targets of examination. In the same figure, the relationships between Eqs. (11) and (12), for which the k_h in the Recommendations is inversely proportional to the 1/2 power of the pile head displacement, are indicated by a broken line, while the power approximation equation (Eq. (13)) based on the least-squares method is indicated by a solid line.

$$(y>0.1y_0) \quad k_h/k_{h0}=(y/y_0)^{-1/2} \tag{11}$$

$$(y\leq 0.1y_0) \quad k_h/k_{h0}=3.16 \tag{12}$$

$$k_h/k_{h0}=a(y/y_0)^x \tag{13}$$

Here, y(m) is the pile head displacement; y_0 is the reference displacement (0.01m); a is a coefficient; and x is an index related to the non-linearity of the coefficient of subgrade reaction. As shown in Fig.8, if the ground deformation coefficient is assessed using Eq. (2), the variation of the cohesive soil is large, and the assessment line in the Recommendations is close to the lower limit of the data. When regression is done on the test data in Eq. (13), a is 2.0 and 2.9 and x is −0.65 and −0.86, and both values are larger than those in the Recommendations (where a=1.0, x=−0.5).

Fig.9 shows the relationship between the inversed k_h/estimated k_{h0} calculated from Eq. (1) and Eq. (10), and the pile head displacement (y) or the pile head displacement/pile diameter (y/B) including both sandy soil and cohesive soil. The k_{h0} in the Recommendations is inversely proportional to 3/4 the power of the pile diameter (Eq. (1)). This is based on the results of the plate loading test in the horizontal direction conducted by *Yoshinaka*[3]. Eq. (1) has been deduced by using a plate loading test with a diameter of 30 cm as the reference[3]. When performed in such a manner that $B/B_0^{-1/2}$, $B/B_0^{-3/4}$, and B/B_0^{-1} become the same at B=30cm, Eqs. (14)-(16) are obtained. These were employed for an assessment of the estimated k_{h0}, to examine the dependence of the pile diameter in Fig.9.

$$k_{h0}=34E_S(B/B_0)^{-1/2} \tag{14}$$

$$k_{h0}=80E_S(B/B_0)^{-3/4} \tag{15}$$

$$k_{h0}=187E_S(B/B_0)^{-1} \tag{16}$$

In addition, the power approximation equation, based on the least-squares method of Eq. (13) and Eq. (17) below, and the correlation coefficient R thereof are both shown in Fig.9.

$$k_h/k_{h0}=a\{(y/B)/(y/B)_0\}^x \tag{17}$$

Here a is a coefficient; $(y/B)_0$: y/B (=0.01) serves as the reference level; and x is an index related to the non-linearity of the k_h. In the Recommendations, a is 1.0 and x is −0.5 in Eq. (13), but when regression is performed for the horizontal load test data, a is 0.97-1.74 and x is −0.59 to −0.68 in Eq. (13), and a is 0.97-1.77 and x is −0.45 to −0.58 in Eq. (17).

An effect owing to the fact that the measured value for the shear wave velocity is not employed is also plausible, but from Fig.9 the overall variation is smaller when the estimated k_{h0} is calculated with the ground deformation coefficient set at $E_S=E_0/18$ than in the method suggested in the Recommendations, as shown in Fig.8. The largest correlation coefficient R of the power approximation equation is $n=-1/2$ when the horizontal axis is used as the y, and is $n=-1$ when the horizontal axis is used as the y/B. The correlation coefficient is somewhat larger when the horizontal axis is used as the y/B rather than the y, and the variation is the lowest in this case. It is recommended that the k_h in the Recommendations be assessed using a non-linear shape that is inversely proportional to the half the power of the y. The k_h in the power approximation equation shown in Fig.9 is dependent on a −0.44 to −0.72 power of the y or the y/B.

From the above results, the condition when the variation is smallest is the −1 power of the pile diameter in the y/B, and the slope is larger than the Recommendations by about the −0.6 power. In addition, the vertical axis becomes 1.0 when the horizontal axis is approximately 0.03 (3%).

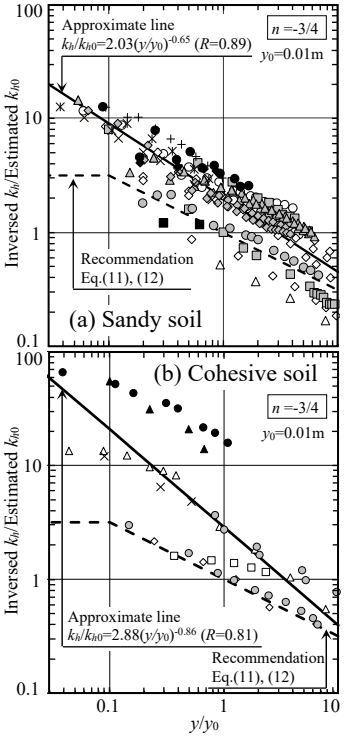

Fig.8 Relationships between inversed k_h/estimated k_{h0} and y/y_0 (700N)

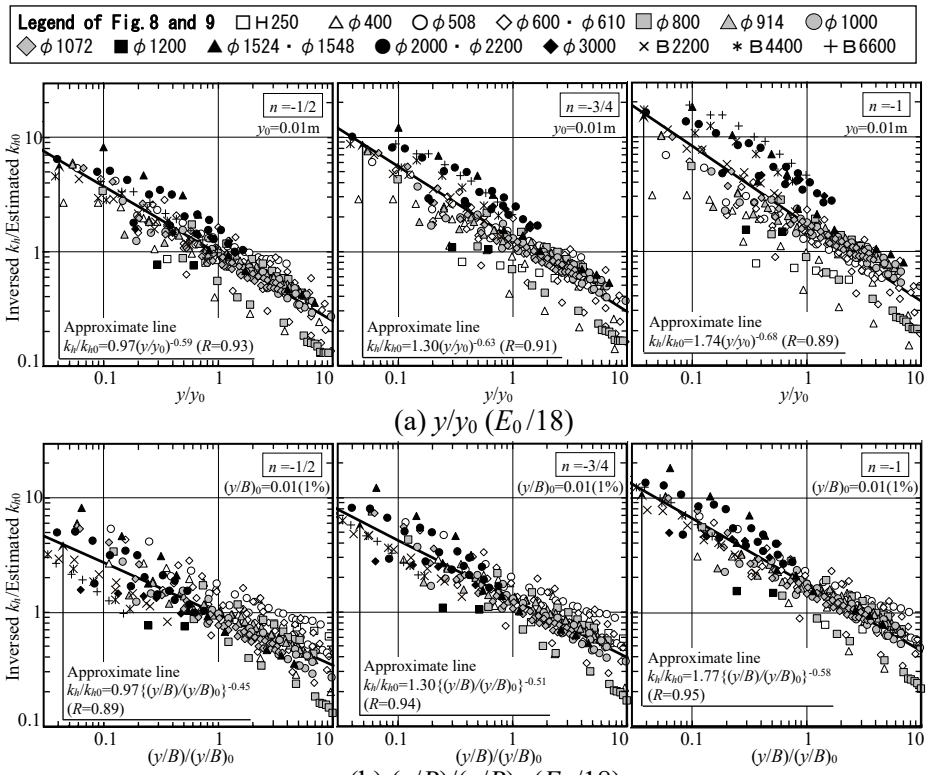

Fig.9 Relationships between inversed k_h/estimated k_{h0} and y/y_0 or $(y/B)/(y/B)_0$

4. The assessment of the coefficient of subgrade reaction using the proposal of Francis and a hyperbolic model

In the seismic design of piles by dynamic stress analysis, a continuous assessment of the coefficient of subgrade reaction k_h from small displacement to large displacement is ideal, and usually this assessment is performed using Eq. (18)[2] (proposed by Francis) and the hyperbolic model.

$$k_{h0}=\frac{1.3}{B}\frac{E_S}{1-\nu^2}\left(\frac{E_S B^4}{EI}\right)^{1/12} \tag{18}$$

Here, B(m) is the pile diameter; ν is Poisson's ratio of the ground (sandy soils : 0.3, cohesive soils : 0.45); E_S(kN/m^2) is the ground deformation coefficient; E(kN/m^2) is Young's modulus of the pile; and I(m^4) is the moment of inertia of area of the pile.

Fig.10 shows the results when the estimated k_{h0} in Fig.9 is calculated using Eq. (18). The power approximation equation based on the least-squares method of Eq. (13) and Eq. (17) and the correlation coefficient R are both noted in the same figure. Since *Francis*' proposal is based on the theory of elasticity, a ground deformation coefficient E_0 employing the V_S was adopted. The variation is smaller when the horizontal axis is ordered by the y/B, to the same extent as the results in Fig.9, wherein the horizontal axis was ordered by the y/B and the −1 power of the pile diameter. The k_h for this power approximation equation is dependent on a -0.52 power for the y/B, and this is close to the value of the Recommendations.

A model that expands the hyperbola has been proposed as the method of calculation of the dynamic deformation characteristics of the ground by *Kokusho et al.*[16]. In this paper, Eq. (19) was used in order to apply *Kokusho*'s proposal to the calculation of the k_h.

$$k_h/k_{h0} = \frac{1}{1+\{(y/B)/(y/B)_r\}^{\alpha}} \tag{19}$$

Here, k_h(kN/m^3) is the coefficient of subgrade reaction; k_{h0}(kN/m^3) is the reference coefficient of subgrade reaction; y/B is the pile head displacement/pile diameter; $(y/B)_r$: y/B at which k_h/k_{h0}=0.5; and α is the index. The results of approximation using the least-squares method employing Eq. (19) shown in Fig.10b) were $(y/B)_r$=0.001, α=0.69 and correlation coefficient R=0.91.

Fig.11 shows a comparison of the power approximation equation of Fig.10b) and Eq. (19). Moreover, Fig.12 shows the relationship obtained by multiplying y/B by the vertical axis in Fig.11 and using this as the value corresponding to the pile head load. A calculation that uses α=2/3 in Eq. (19) is also shown in these figures. From Fig.11, the calculation based on Eq. (19) exhibits a generally good agreement with the power approximation equation, even though there is a tendency for it to be under-estimated in the small strain region. On the one hand, when the approximation equation based on the least-squares method of Eq. (19) is compared with the power approximation equation in Fig.12, the difference of the y/B at the same load level is small in the region where the y/B is small, but it becomes larger in the large y region. On the other hand, in the assessment that uses α=2/3, the agreement with the power approximation equation improves in the region of large y/B, more than in the approximation equation based on the least-squares method in Eq. (19).

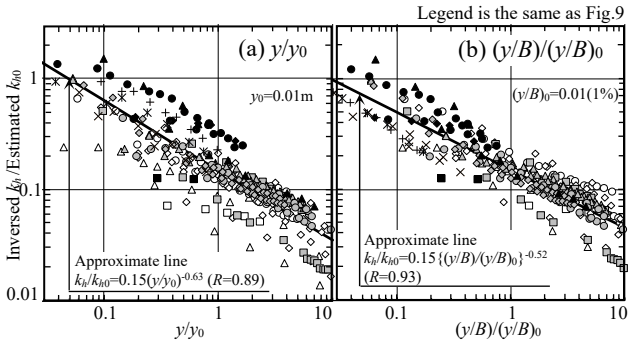

Fig.10 Relationships between inversed k_h/estimated k_{h0} (*Francis*' proposal, E_0)

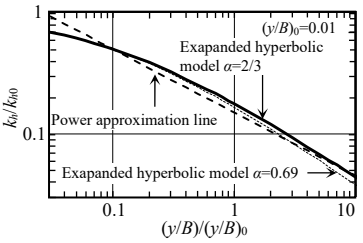

Fig.11 Relationships between k_h/k_{h0} and $(y/B)/(y/B)_0$ (Expande hyperbolic model)

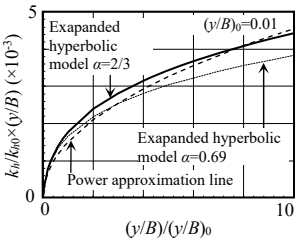

Fig.12 Relationships between $k_h/k_{h0}(y/B)$ and $(y/B)/(y/B)_0$

5. Simulation analysis

A simulation analysis using the theoretical solution was conducted with the tests shown in Table 1. As shown in Table 2, three conditions were used, the conditions of Fig.8 (Case1),the y/B and $(B/B_0)^{-1}$ at which the variation was small in Fig.9 (Case2), and the coefficient of subgrade reaction proposed by *Francis* in Fig.11 (Case3). For the dependence of the y or y/B on the coefficient of subgrade reaction k_h, Eqs. (11) and (12) were adopted by Case1, Eq. (17) was adopted by Case2, and Eq. (19) was adopted by Case3. In Case2 the values were set at $(y/B)_0$=0.03, coefficient a=1.0, and index x=−0.6. In Case3 the values were set at $(y/B)_r$=0.001 and α=2/3.

As examples of the analysis results, Fig.13 shows the relationship between the pile head load and the pile head displacement in the sandy soil 2 test (S11, S16) and cohesive soil 2 test (C11, C15). In the same figure, the measured value after the pile yields is also shown, the data is shown in black (●) when the pile is within the elasticity range and in gray (●) after the yield. Before plasticizing of the pile, the methods employing the shear wave velocity (Case2-3) exhibit relatively good agreement with the measured values compared to Case1 (the Recommendations), and no significant differences can be found in Case2-3.

Among the results of all cases, Fig.14 shows a comparison of the pile head displacement when the pile is within the elasticity range, and the measured values for the max. bending moment (M_{max}). The M_{max} was obtained in the sandy soil 8 test and cohesive soil 6 test shown in Fig.1. Moreover, since the measured values of the M_{max} are not shown at all pile head loads, the data have been excluded in part. The variation of the pile head displacement is extremely large in Case1. Although the variation is large in Case2-3, which employ shear wave velocity, the measured values mostly correspond on average, as long as the slopes of the approximation line are observed to be 1.0. In addition, with regard to the M_{max} of Case1-3, variation to the extent of the pile head displacement is not observed, and the slopes of the regression lines are all in the range 0.9-1.1.

As examples of the bending moment distribution, Fig.15 shows the S10 and C11 results. In Case1, the depth at which the M_{max} occurred is deeper than in Case2-3, and a tendency for the M_{max} to become larger along with this was also observed. On the other hand, the M_{max} of Case2-3 were more or less the same, and were under-assessed compared to the measured values.

Table2 Simulation analysis conditions

Case	E_S Sandy soil	E_S Cohesive soil	k_{h0}	k_h/k_{h0}	Ref. disp. at k_{h0}	Legend of Fig.13
1	700N		Eq.(15)	Eq.(11)(12)	y_0=1cm	---+---
2	E_0/18		Eq.(16)	Eq.(17)	$(y/B)_0$=3% a=1.0 x=−0.5	□
3	E_0		Eq.(18)	Eq.(19)	$(y/B)_r$=0.1% α=2/3	△

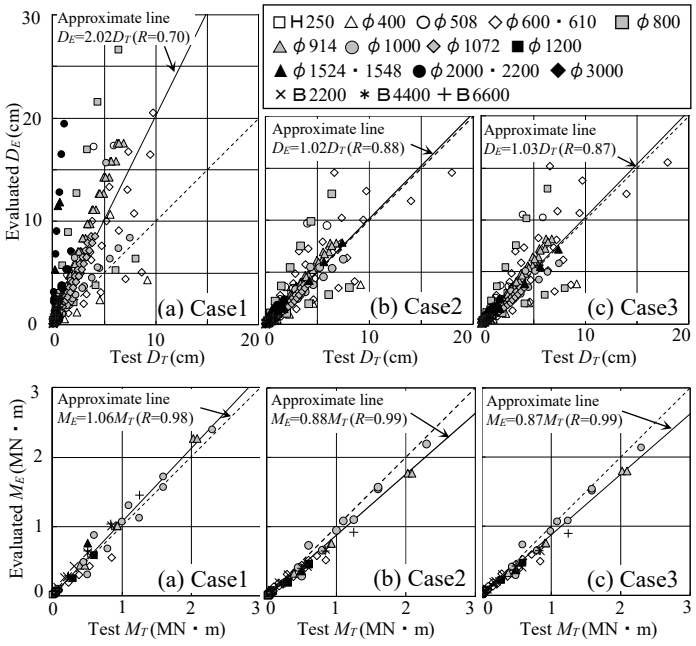

Fig.14 Comparisons of displacement D at pile head and max. bending moment M between test data and evaluated data

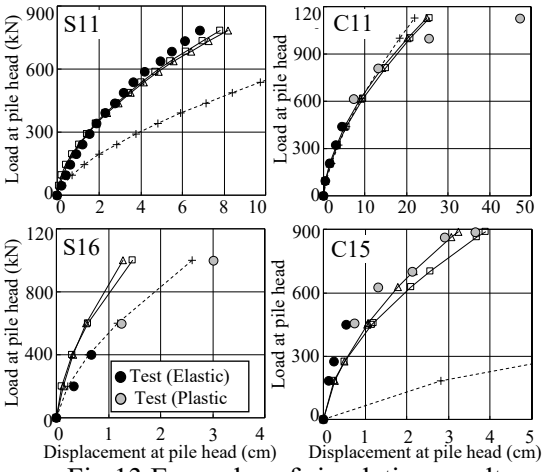

Fig.13 Examples of simulation results

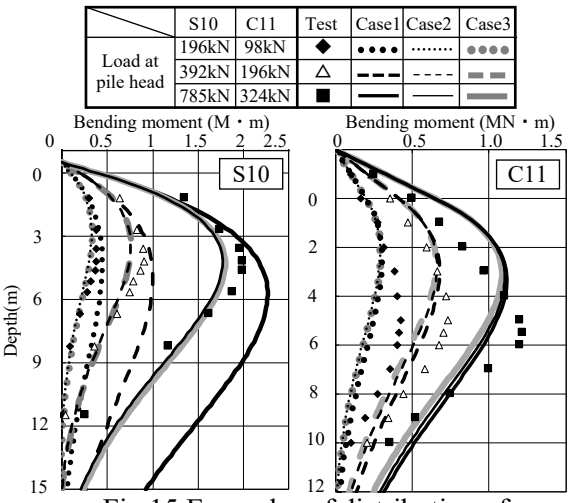

Fig.15 Examples of distribution of bending moment

6. Proposal of the assessment method

From the results thus far, two methods are proposed to assess the ground deformation coefficient and coefficient of subgrade reaction employed in the theoretical solution. Fig.16 shows proposed method and the relationship between the inversed k_h/estimated k_{h0} and $(y/B)/(y/B)_0$ or $(y/B)/(y/B)_r$. The estimated k_{h0} is calculated using methods A and B.

Method A	Method B
$k_{h0}=187E_S(B/B_0)^{-1}$ (20)	$k_{h0}=\frac{1.3}{B}\frac{E_S}{1-\nu^2}\left(\frac{E_S B^4}{EI}\right)^{1/12}$ (24)
$k_h/k_{h0}=\{(y/B)/(y/B)_0\}^{-0.6}$ (21)	$k_h/k_{h0}=\frac{1}{1+\{(y/B)/(y/B)_r\}^{2/3}}$ (25)
$k_{h,max}=18k_{h0}$ (22)	$E_S=E_0$ (26)
$E_S=E_0/18$ (23)	

E_S(kN/m^2) is the ground deformation coefficient; E_0(kN/m^2) is the initial deformation coefficient of the ground calculated from the shear wave velocity; k_{h0}(kN/m^3) is the reference coefficient of subgrade reaction; y(m) is the pile head displacement; B(m) is the pile diameter; B_0 is the pile width that serves as the reference level (0.01m); $(y/B)_0$ is 0.03; $k_{h,max}$(kN/m^3) is the maximum coefficient of subgrade reaction; ν is Poisson's ratio of the ground; E(kN/m^2) is Young's modulus of the pile; I(m^4) is the moment of inertia of area of the pile; and $(y/B)_r$=0.001.

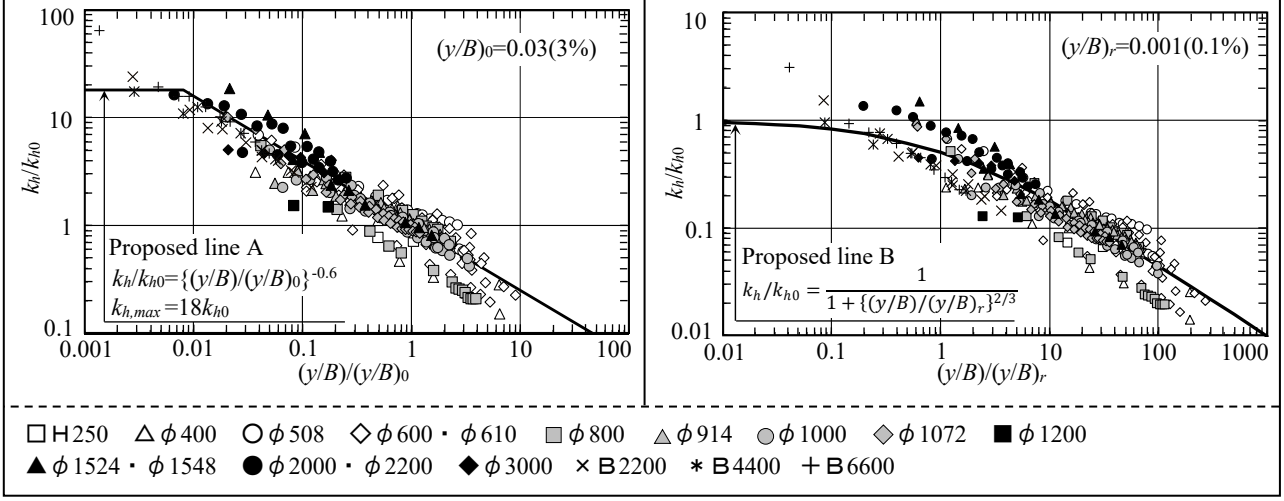

Fig.16 Proposed methods

In method A, the relationship is such that k_h/k_{h0}=1 with $(y/B)/(y/B)_0$=1.0, while in method B k_h/k_{h0}=0.5 with $(y/B)/(y/B)_r$=1, and this shows good agreement over a wide range with the measured values. In particular, since method B can provide continuous assessment (from small displacement to large displacement), it is a highly versatile method that can be used in static and dynamic stress analysis.

7. Conclusions

In this study, a method for assessing the coefficient of subgrade reaction k_h from the initial stiffness of the ground to failure was investigated using an examination of the effects of the strain level of the ground with pressuremeter test and an inversed analysis of horizontal load test results with the theoretical solution. The findings obtained were as follows:

1) A method for assessing the strain dependence of the ground deformation coefficient, which is employed in the assessment of the coefficient of subgrade reaction, was determined. In addition, a ground deformation coefficient assessment independent of the soil type was performed by adopting shear wave velocity.
2) With regard to the non-linearity of the coefficient of subgrade reaction k_h, the fact that continuous changes with small variation could be assessed using the pile displacement/pile diameter, and the fact that the strain level of the ground could be considered throughout, were clarified.
3) An assessing method for the coefficient of subgrade reaction k_h continuously from small strain to large strain, that can be used in dynamic analysis, with the springs proposed by *Francis* based on the theory of elasticity and with expanded hyperbolic model, was proposed.

8. References

[1] A. B. Vesic (1961): Bending of Beams Resting on Isotropic Elastic Solid, *Journal of the Engineering Mechanics Division*, ASCE, Vol.87, No.EM2, 35-53.

[2] A. J. Francis (1964): Analysis of Pile Groups with Flexural Resistance, *Journal of the Soil Mechanics and Foundation Division*, ASCE, Vol.90, No.SM3, 1-32.

[3] Yoshinaka, R. (1967): Coefficient of Subgrade Reaction Considering Scale effect, *Technical Note of Public Works Research Institute*, No.299 (in Japanese).

[4] Architectural Institute of Japan (2019): Recommendations for Design of Building Foundations, 270-277 (in Japanese).

[5] Y. L. Chang (1937): Discussion on “Lateral Pile Loading Tests” by L. B. Feagin, A.S.C.E Transaction Vol.102, 272-278

[6] Architectural Institute of Japan (1990): Ultimate Strength and Deformation Capacity of Building in Seismic Design (1990), 164 (in Japanese).

[7] Shimomura, S. and Suzuki, Y. (2016): Coefficient of Subgrade Reaction Estimated from Horizontal Load Test Data of Single Piles with Wide range Diameter in Sand Deposit, *AIJ Journal of Technology and Design*, Vol.22, No.52, 919-924 (in Japanese).

[8] Shimomura, S. and Suzuki, Y. (2017): Coefficient of Subgrade Reaction Estimated from Horizontal Load Test Data of Single Piles with Wide range Diameter in Cohesive Soil Deposit, *AIJ Journal of Technology and Design*, Vol.23, No.53, pp.93-98 (in Japanese).

[9] JGS 1531-2012 (2012): Pressuremeter test to evaluate index of the ground, *Japanese Geotechnical Society*.

[10] Tabei, T., Uchida, A., Kobayashi, H. and Hatanaka, M. (2011): Strain Level of Deformation Modulus for Cohesive Soils Obtained by Soil Investigation, *Summaries of Technical Papers of Annual Meeting, Architectural Institute of Japan*, Structure- Ⅰ, 413-414 (in Japanese).

[11] Koyamada, K., Miyamoto, Y. and Miura, K. (2003): Nonlinear Property for Surface Strata from Natural Soil Samples, *38th Japan National Conference on Geotechnical Engineering*, 2077-2078 (in Japanese).

[12] Imazu, M. and Fukutake, K. (1986): Dynamic Shear Modulus and Damping of Gravel Materials, *21th Japan National Conference on Geotechnical Engineering*, 509-512 (in Japanese).

[13] Hara, A. (1980): Dynamic Characteristics of Soils and Response Analysis of Soil Deposits, *Doctoral Thesis*, University of Tokyo (in Japanese).

[14] Japan Road Association (2012): Specifications for Highway Bridges, Part Ⅴ Seismic Design, 32-33 (in Japanese).

[15] Imai, T. (1977): P- and S-Wave Velocities of the Ground in Japan, *Proceedings of the 9th International Conference on Soil Mechanics and Foundation Engineering*, Vol.2, 257-260.

[16] Kokusho, T. and Motoyama, R. (1998): Application of Equivalent Linear Analysis to Large Strain Problems (Formulation for Strain-Dependency of Shear Modulus Ratio and Damping Ratio), *33th Japan National Conference on Geotechnical Engineering*, 773-774 (in Japanese).

